Calorimetric Investigation of Triazole-Bridged Fe(II) Spin-Crossover One-Dimensional Materials: Measuring the Cooperativity

ARTICLE *in* THE JOURNAL OF PHYSICAL CHEMISTRY B · MARCH 2011

Impact Factor: 3.3 · DOI: 10.1021/jp109489g · Source: PubMed

5 AUTHORS, INCLUDING:

Miguel Castro
University of Zaragoza
69 PUBLICATIONS **1,243** CITATIONS
SEE PROFILE

Ramon Burriel
Spanish National Research Council
166 PUBLICATIONS **1,784** CITATIONS
SEE PROFILE

Jaap G Haasnoot
Leiden University
288 PUBLICATIONS **8,022** CITATIONS
SEE PROFILE

Jan Reedijk
Leiden University
1,375 PUBLICATIONS **38,157** CITATIONS
SEE PROFILE

THE JOURNAL OF PHYSICAL CHEMISTRY B

ARTICLE

pubs.acs.org/JPCB

Calorimetric Investigation of Triazole-Bridged Fe(II) Spin-Crossover One-Dimensional Materials: Measuring the Cooperativity

Olivier Roubeau,*[,†,‡] Miguel Castro,[†] Ramón Burriel,[†] Jaap G. Haasnoot,[‡] and Jan Reedijk[‡,§]

[†]Instituto de Ciencia de Materiales de Aragón, CSIC and Universidad de Zaragoza, Plaza San Francisco s/n, 50009 Zaragoza, Spain

[‡]Leiden Institute of Chemistry, Leiden University, P.O. Box 9502, 2300 RA Leiden, The Netherlands

[§]Department of Chemistry, King Saud University, P.O. Box 2455, Riyadh 11451, Saudi Arabia

Supporting Information

ABSTRACT: The relevance of abrupt magnetic and optical transitions exhibiting bistability in spin-crossover solids has been pointed out for their potential applications in optical or memory devices. In this respect, triazole-based one-dimensional coordination polymers are widely recognized as one of the most interesting systems. The measure of the interaction among spin-crossover centers at the origin of such cooperative behavior is of paramount importance and has so far been realized through modeling of spin-crossover curves derived mostly from magnetic measurements. Here, a new series of triazole-based one-dimensional coordination polymers of formula $[Fe(Rtrz)_3](A)_2 \cdot xH_2O$ with R = methoxyethyl and A = monovalent anion has been prepared that show complete and abrupt spin-crossover phenomenon as shown by magnetic measurements. The spin-crossover transition in these and related compounds is studied by differential scanning calorimetry, and the thermodynamic excess enthalpies and entropies associated with the phenomenon are derived systematically. Then the cooperative character of the spin-crossover in these materials is quantified by use of two widely used models, so-called Slichter and Drickamer and domain models. The same procedure is applied to spin-crossover curves of similar compounds available in the literature and for which calorimetric studies have been reported. The experimental thermodynamic figures, in particular the excess enthalpies, are shown to be clearly correlated to the output parameters of both models, thus providing a direct, experimental, quantitative measure of the cooperative character of the spin-crossover phenomenon.

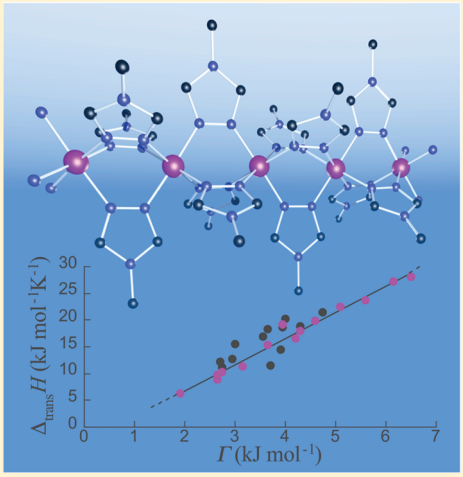

INTRODUCTION

Phase transitions in condensed matter manifest themselves as concerted effects of molecular structure and motions and intermolecular interactions. Because calorimetry is very sensitive to such changes in the degree of short-range or long-range order in the condensed states of matter, it is a very powerful tool to detect and study phase transitions and therefore to better understand materials. This is particularly true for molecular-based magnetic materials.[1] Spin-crossover (SCO) solids are molecular-based materials experiencing thermally induced phase transitions in which a change in the electronic state is strongly coupled with lattice transformations.[2] In six-coordinate Fe(II) spin-crossover compounds, the reversible transition from low-spin diamagnetic state (LS, $^1A_{1g}$, $S = 0$) to high-spin paramagnetic state (HS, $^5T_{2g}$, $S = 2$) is often accompanied by a thermochromic effect, making them a very attractive class of switchable molecular systems.[3] Although the phenomenon has been extensively studied, in particular systems of Fe(II),[2b−d] and the primary driving force governing the spin conversion is the entropy increase arising from differences in spin multiplicity and density of vibrational states between LS and HS states, calorimetric studies on series of similar compounds are still relatively scarce.[4] The first detailed calorimetric study by Sorai and Seki[4a] on $[Fe(phen)_2(NCX)_2]$ (X = S, Se) proved the presence of strong cooperative intermolecular interactions, proceeding via significant coupling between the electronic state and the phonon system, and that these were at the origin of the sharp heat capacity peaks observed. This stems from the large difference in metal−ligand bond length and the concomitant volume variation of the spin-changing molecules upon the SCO transition.[5] The strength of these intermolecular interactions, which have been shown to be merely of elastic origin,[6] decides whether the SCO system is of the "abrupt-type", that is, with the spin state conversion occurring within a narrow temperature range (typically < ∼10 K), or of the "gradual-type", that is, with the spin state conversion taking place over a much wider range. In the latter case, no sharp heat capacity peak is observed. In most cases studied, which are merely zero-dimensional complexes, larger excess enthalpies

Received: October 3, 2010
Revised: February 5, 2011
Published: March 07, 2011

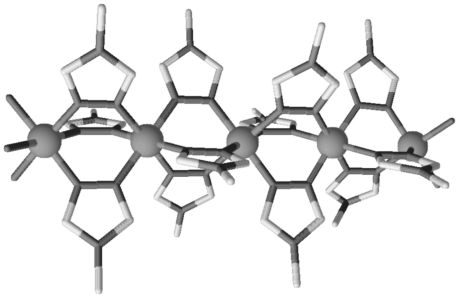

Figure 1. Perspective view of successive triple 4-R-1,2,4-triazole bridges between iron(II) ions resulting in a linear $[Fe(Rtrz)_3]_n^{2n+}$ chain. The three-dimensional structure was minimized with R = methyl in ACD Chemsketch 12.0. Carbon, nitrogen, and iron atoms are respectively depicted as white sticks, gray sticks, and gray balls.

and entropies due to the spin transition were found in abrupt-type systems (8−10 kJ mol^{-1} and 50−70 J mol^{-1} K^{-1}, respectively),[4,7] than in gradual-type ones (4−8 kJ mol^{-1} and 25−40 J mol^{-1} K^{-1}, respectively).[4,8] In particular, the excess entropy not due to the change in spin manifold, which is mainly ascribed to changes in internal vibrations, has been found to qualitatively reflect the cooperative character of the spin transition phenomenon.

Cooperative 1,2,4-triazole-based chainlike polymeric SCO compounds of formula $[Fe(Rtrz)_3](A)_2 \cdot xH_2O$ (see Figure 1, with R = 4-substituent, and A = monovalent anion), which are potentially applicable in optical or memory devices,[9] exhibit abrupt reversible spin transitions accompanied by a change of color from white (HS) to purple (LS), and can be implemented into soft-matter phases such as gels, Langmuir−Blodgett films, or nanoparticles dispersions.[10] The completeness of the transitions is dependent on the size of the polymeric chains,[11] and the transition temperatures can be controlled through the counterion and the 4-substituent on the triazole ligands.[9c,d,11,12] Hysteresis effect is usually observed, in particular with small substituents. The linear chainlike structure of these materials, as shown schematically in Figure 1, has been deduced from X-ray absorption experiments,[13] since no crystal structure could be solved so far. The structures of a limited number of Cu(II) compounds of similar formula have been solved, supporting this structural model.[12c,14] Extremely large excess enthalpy (28 kJ mol^{-1}) and entropy (80 J K^{-1} mol^{-1}) due to the spin transition have been measured in $[Fe(Htrz)_2trz](BF_4)$;[15] such high figures are thought to be a consequence of both strong intrachain interactions, arising from direct rigid chemical link between the Fe(II) ions (see Figure 1) and interchain (e.g., intermolecular) interactions. Indeed, a theoretical model contemplating elastic long and short-range interactions showed that both extremely strong intrachain and additional long-range interactions are necessary to reproduce the 50 K wide hysteresis exhibited by the latter compound.[16] This compound is considered to be very peculiar because of its charged triple triazole bridge and the strong hydrogen bonding between the BF_4^- anions and the triazolate ligands. Hence, it is unclear whether any chainlike material possessing uncharged triple triazole bridges would possess the same intrachain strong interactions. On the other hand, it is clear that the presence and the nature of the substituent on the triazole rings will trigger the intermolecular interactions between the polymeric chains. This family of compounds, in which the cooperative character of the SCO as well as its

Scheme 1. Schematic Representation of the Ligands and Abbreviations Used or Discussed in This Work

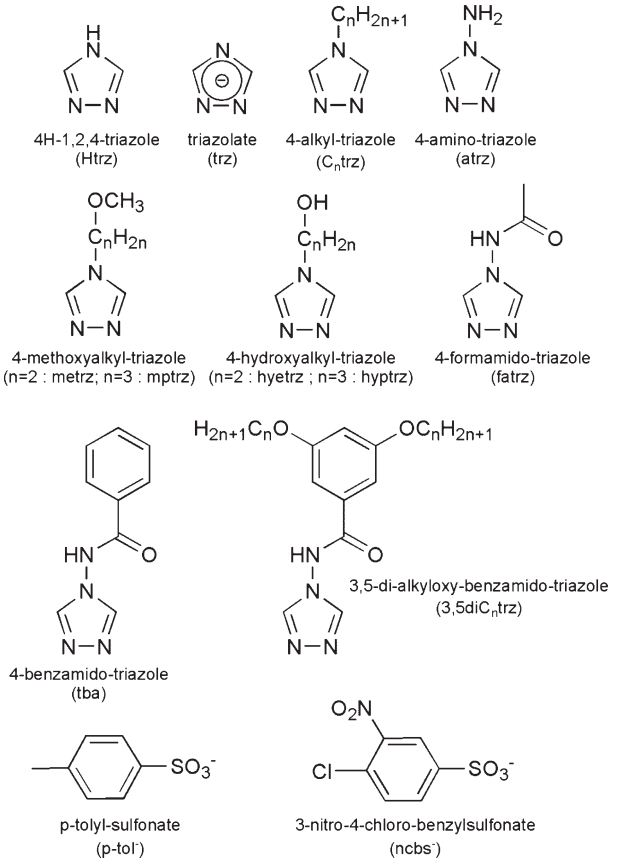

temperature range can be varied without significant variation of the chemical formula or structural type, provides a unique opportunity to quantitatively estimate the cooperativity and correlate it to thermodynamic parameters of the SCO.

For this purpose, a new series of such $[Fe(Rtrz)_3](A)_2 \cdot xH_2O$ polymeric materials with R = methoxyethyl (mxetrz) has been synthesized and is reported here, namely **1** with A = BF_4^- and x = 2, **2** with A = ClO_4^- and x = 2, **3** with A = NO_3^- and x = 1, **4** with A = $C_7H_7SO_3^-$ (p-tol$^-$) and x = 2, and **5** with A = $CF_3SO_3^-$ (triflate) and x = 2. Magnetic and calorimetric characterizations of this series are presented here. Previously reported compounds of the same family, namely a tetrafluoridoborate member (**6**, with R = butyl and x = 2), a triflate-containing series with x = 2 and R = n-alkyl groups with m carbon atoms[11] (**7**, m = 5, **8**, m = 7, **9**, m = 10 and **10**, m = 13), and a series based on the 4-formylamino-triazole (fatrz)[9d] (**11** with A = $CF_3SO_3^-$ and x = 2, **12** with A = p-tol$^-$ and x = 2, **13** with A = BF_4^- and x = 2, **14** with A = NO_3^- and x = 1) have also been reinvestigated by calorimetry. To correlate thermodynamic figures derived from calorimetric measurements and parameters describing the SCO, all such reported data on $[Fe(Rtrz)_3](A)_2 \cdot xH_2O$ compounds (see Scheme 1 for the R substituents) in the literature are also gathered. The SCO curves for all these related compounds are analyzed with two widely used models that provide a quantitative measure of the cooperative character of the SCO. The excess enthalpies associated with the SCO are shown to correlate with both model parameters, thus providing a quantitative experimental measure of cooperativity.

EXPERIMENTAL SECTION

Synthesis. Iron(II) tetrafluoridoborate and perchlorate hexahydrates were purchased from Aldrich and Ventron respectively, and were used without further purification. Iron(II) trifluoromethylsulfonate and *p*-toluenesulfonate were obtained by warming iron powder (Acros) and the corresponding acid (Aldrich) in water. The nitrate salt was prepared from the reaction of iron sulfate (Aldrich) with a 20% excess of barium nitrate (Merck). The barium sulfate precipitate that formed was filtered and the aqueous solution of iron nitrate used right away.

The 4-methoxyethyl-1,2,4-triazole (mxetrz) was obtained in a 40% yield from 1-amino-2-methoxy-ethane (Acros) following the general route described by Bayer et al.[17] ^{1}H NMR (d^6-dmso, 200 MHz): δ = 8.40 ppm (2H), δ = 4.19 ppm (t, 2H), δ = 3.58 ppm (t, 2H), δ = 3.22 ppm (3H). IR (neat): ν = 634 (γ_{C-H} ring torsion), 868 (γ_{C-H} out of plane), 1117 (ether COC antisymmetric), 1189 (γ_{N-N}), 1383, 1458, and 1536 (ring stretches), 2938 (ν_{C-H} aliphatic), 3120 (ν_{C-H} aromatic) cm^{-1}. Anal. Calcd (found) for $C_5H_9N_3O$: C, 47.2 (46.8), 7.1 (7.2), 33.0 (33.3).

Compounds **1** to **5** were synthesized as follows: a hot ethanolic solution (3.5 mmol, 10 mL) of mxetrz was added slowly to a hot aqueous solution of the desired iron(II) salt (1 mmol, 10 mL). Ascorbic acid was added in small quantities in all syntheses to prevent oxidation to iron(III). Compounds **1** to **5** precipitated upon cooling, within an hour. The precipitates were left aging a minimum of one hour before filtration and washed with absolute ethanol and diethyl ether. Upon drying in air, the nitrate and p-tol$^-$ compounds **3** and **4** turned purple, indicating the presence of iron(II) low spin species. The other three compounds were isolated as white solids. Anal. Calcd (found) for $[Fe(mxetrz)_3](BF_4)_2\cdot 2H_2O$ (**1**): C, 27.8 (27.5); H, 4.8 (4.7); N, 19.5 (19.6). Anal. Calcd (found) for $[Fe(mxetrz)_3](ClO_4)_2\cdot 2H_2O$ (**2**): C, 26.8 (26.3); H, 4.6 (4.5); N, 18.7 (18.9). Anal. Calcd (found) for $[Fe(mxetrz)_3](NO_3)_2\cdot H_2O$ (**3**): C, 31.1 (30.6); H, 5.0 (4.7); N, 26.6 (26.6). Anal. Calcd (found) for $[Fe(mxetrz)_3](C_7H_7SO_3)_2\cdot 2H_2O$ (**4**): C, 42.7 (42.1); H, 5.6 (5.3); N, 15.5 (15.8); S, 7.9 (7.4). Anal. Calcd (found) for $[Fe(mxetrz)_3](CF_3SO_3)_2\cdot 2H_2O$ (**5**): C, 26.5 (25.9); H, 4.0 (3.9); N, 16.3 (16.7); S, 8.3 (7.8)

Syntheses and analysis of compounds **6**−**14** have been described elsewhere.[9d,11] Repeated synthesis of identical compounds showed reproducible magnetic behavior, except for compound **6**, as detailed in the text and Supporting Information Figure S2. The determination of the amount of water is subject to large errors, solely based on the elemental analysis, and thermogravimetric measurements were used to confirm the amount of water molecules. All compounds described in this work are stable in air at 20 °C.

Magnetic Measurements. Bulk magnetization of powder samples was measured using Quantum Design SQUID magnetometers, either MPMS-5S (Leiden) or MPMS-XL (Zaragoza). The applied field for temperature-dependent measurements was 0.1 T in the range of linear dependence of *M* versus *H*. The measured values were corrected for the experimentally measured contribution of the sample holder, while the derived susceptibilities were corrected for the diamagnetism of the samples, estimated from Pascal's tables.[18] Warming and cooling rates were of the order of 0.3 K min^{-1}. Note that the measurements are performed, after purging, under a reduced pressure of He, which is of importance for the behavior of compounds **4**, **11**, **12**, and **14** that are subject to water loss.

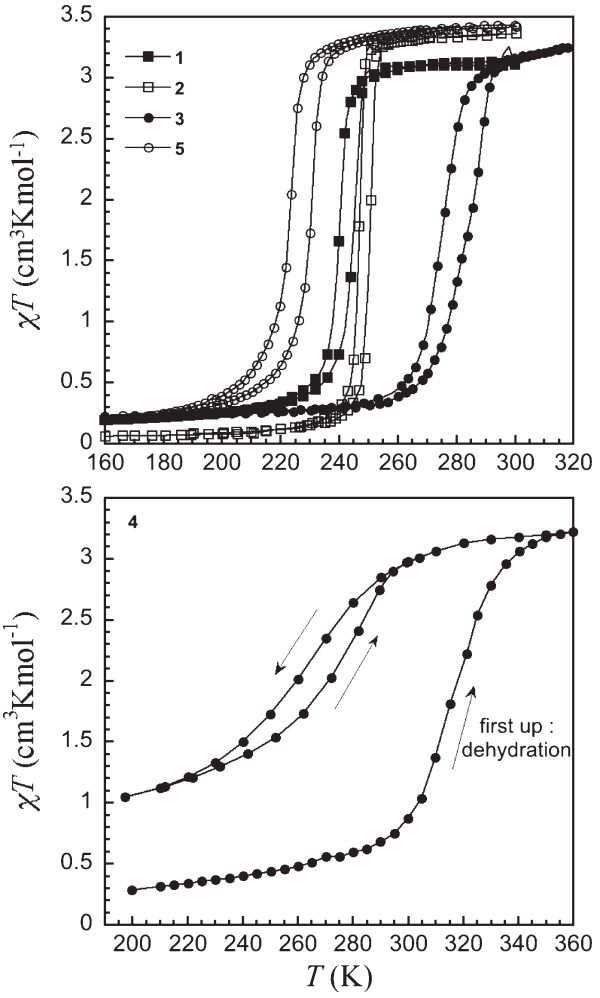

Figure 2. Temperature dependence of the product χT of the polymeric compounds with methoxyethyltriazole. (Top) BF_4^- (**1**), ClO_4^- (**2**), NO_3^- (**3**), and triflate (**5**) anions; (Bottom) p-tol$^-$ (**4**) anion.

Differencial Scanning Calorimetry (DSC). Heat capacities were obtained by use of either a Perkin-Elmer DSC-7 instrument or a differential scanning calorimeter Q1000 with the LNCS accessory from TA Instruments. The temperature and enthalpy scales were calibrated by using the melting (279.69 K, 2678 J mol^{-1}) and crystal-to-crystal (186.10 K, 6740 J mol^{-1}) transitions of cyclohexane with the DSC-7 instrument or with a standard sample of indium, using its melting transition (156.6 °C, 3296 J mol^{-1}), for the Q1000 apparatus. The measurements were carried out using 3−15 mg of powdered samples sealed in aluminum pans with a mechanical crimp with an empty pan as reference. When using the TA Instruments Q1000, the zero-heat flow procedure described by TA Instruments was followed, using synthetic sapphire as reference compound. When using the Perkin-Elmer DSC-7 instrument, the empty aluminum pan was measured in the exact same conditions prior to filling, thermal equilibrium was checked at starting and final temperatures of each scan by 4 min isotherms and the isothermal edges were linearly transformed to the same origin. A synthetic sapphire sample of comparable mass to the used samples was also measured to ensure the accuracy of the heat-capacity results. These steps correspond to the well-known procedure to obtain the massic heat capacity of a sample from

Table 1. Transition Parameters of the Spin Transition in Compounds 1−14

compound	$T_{1/2}{}^{up}$ (K)[a]	$T_{1/2}{}^{down}$ (K)[a]	ΔT_{80} (K)[a]	res HS (%)	Γ/Γ_{up} (kJ mol^{-1})	n_{Sorai}	T^{up} (K)[b]	T^{down} (K)[b]	$\Delta_{trans}H$ (kJ mol^{-1})[e]	$\Delta_{trans}S$ (J mol^{-1} K^{-1})[e]
1, $[Fe(mxetrz)_3](BF_4)_2\cdot 2H_2O$	244	240	6	4	4.65/3.95	10.5	237.5	228.9	18.1	75.0
2, $[Fe(mxetrz)_3](ClO_4)_2\cdot 2H_2O$	251.1	247.1	3	<2	4.75/4.00	21.3	247.1	244.0	20.1	80.5
3, $[Fe(mxetrz)_3](NO_3)_2\cdot H_2O$	283.6	276.2	12	5	5.55/3.55	8.0	298.6	296.4	15.5	51.5
4, $[Fe(mxetrz)_3](p\text{-}tol)_2\cdot 2H_2O$	282	270	60[a]	4			297	287	27.4	94.3
5, $[Fe(mxetrz)_3](CF_3SO_3)_2\cdot 2H_2O$	230.5	224	17	3	4.40/3.70	10.3	228		11.2	36.0
6, $[Fe(C_4trz)_3](BF_4)_2\cdot 2H_2O$	210.5	208.5	46	3	3.95/2.70	3.5	217		9.7	44.7
7, $[Fe(C_5trz)_3](CF_3SO_3)_2\cdot 2H_2O$	227	223	10	<2	4.35/3.65	4.9	228.8	226.5	18.0	77.4
8, $[Fe(C_7trz)_3](CF_3SO_3)_2\cdot 2H_2O$	212	212	50	8	2.75	3.1	229*		10.5	44.7
9, $[Fe(C_{10}trz)_3](CF_3SO_3)_2\cdot 2H_2O$	212	212	20	2	2.95	3.0	216*		12.1	57.8
10, $[Fe(C_{13}trz)_3](CF_3SO_3)_2\cdot 2H_2O$	236	236	45	2	3.00	3.2	244*		15.2	65.9
11, $[Fe(fatrz)_3](CF_3SO_3)_2\cdot 2H_2O$	276	274	8	2	4.80/4.30	16.3	270.7	264.4	17.2	64.3
12, $[Fe(fatrz)_3](p\text{-}tol)_2\cdot 2H_2O$[d]	268	263	50[a]	5			319.4	305.4	20.7	65.3
13, $[Fe(fatrz)_3](BF_4)_2\cdot 2H_2O$	283	283	25	4	3.90	5.9	281.8		13.0	48.3
14, $[Fe(fatrz)_3](NO_3)_2\cdot H_2O$[c]	307	297	20[a]	<2	6.00/4.75	9.9	310.6	308.9	20.1	62.1

[a] From magnetic data: $T_{1/2}$ stands for the temperature at which half of the SCO centers have change their spin; the $T_{1/2}$ and ΔT_{80} of compounds **4**, **12**, and **14** are those of the dehydrated forms. [b] From DSC: the temperatures correspond to the extrapolation at zero scan rate, except where marked by a *, where they correspond to the temperature of the peak maxima observed at 10 K min^{-1}. [c] For compound **14**, only the data corresponding to the main heat capacity peak are given. [d] The DSC data for compound **12** correspond to a modified hydrated form (see text). [e] Excess enthalpies and entropies are given per mole of transition Fe(II) ions: they are corrected of the residual HS fraction evaluated through UV-vis-NIR spectroscopy at low temperature.

experimental heat flows.[19] An overall accuracy of ca. 0.2 K in temperature and up to 5 to 10% in the heat capacity was thus estimated over the whole temperature range. Indeed, small variations between warming and cooling modes of about 5 to 10% in C_p at similar temperatures are detected for some of the compounds studied.

RESULTS AND DISCUSSION

Magnetic Properties. The temperature dependencies of the product χT for compounds **1**-**5**, obtained with 4-methoxyethyl-1,2,4-triazole, are represented in Figure 2 (χ is the magnetic susceptibility per mole of $[Fe(mxetrz)_3](A)_2\cdot xH_2O$ formula unit). They exhibit typical LS ↔ HS transition curves from a value of 0.05−0.3 cm^3 mol^{-1} K at low temperatures to 3−3.4 cm^3 mol^{-1} K at high temperatures. The abruptness of these transition curves is usually considered to be related to the cooperativity exhibited by the compound upon the spin transition and can be evaluated by the temperature range ΔT_{80} in which 80% of the transiting Fe(II) ions undergo their spin transition (see Table 1). The value of χT at low temperatures is indicative of the amount of residual HS centers, which is ascribed to the polymeric chain ends that bear coordinating water molecules and/or monocoordinated triazole ligands. By comparison to trinuclear species[20] possessing the same triple triazole bridges in which only the central iron(II) ions exhibits a spin conversion, these chain ends are expected to remain HS. Therefore the residual paramagnetism at low temperatures is a measure of the actual length of the polymeric chains. An estimation of that residual HS fraction has been obtained on basis of the magnetic susceptibility data and low-temperature UV-vis-NIR absorption spectra (Supporting Information Figure S1). In these estimations, the contribution of temperature independent paramagnetism of LS species was neglected, as previous Mössbauer experiments on this type of materials showed that the values of χT at low temperatures were corresponding merely to the observed HS fraction.[21] The average chain sizes derived are in correct agreement with those derived by dynamic light Scattering in dilute chloroform solutions.[22] A hysteresis effect is observed in all cases with a width of 4−12 K, and the transitions are sharper in the case of BF_4^- (**1**) and ClO_4^- (**2**). In addition, the hysteresis loops of the NO_3^- (**3**) and $CF_3SO_3^-$ (**5**) compounds seem less symmetric. Interestingly, compound **3** is deep purple, merely LS, at 0 °C and white above 25 °C. This is indeed a confirmation of the almost systematic feasibility of obtaining transition temperature(s) in the room temperature range by use of 4-substituted triazoles. The tosylate polymer **4** exhibits a first abrupt spin change centered at ∼315 K, and thereafter much more gradual and partial transitions at lower temperatures, although a hysteresis of 12 K width is then still detected. As previously discussed in literature,[11,23] this is due to a loss of water with the dehydrated form being HS at 300 K while the hydrated form is merely LS. Thermogravimetric analysis confirmed the presence of a loss of water, starting at 310 K and reaching ca. 4.2% (ca. 95% of the water content) at 400 K.

The magnetic and thermogravimetric characterization of compounds **6**−**14** have been reported in previous papers,[9d,11] and only relevant details will be recalled here (see Table 1). In the case of compound **6**, freshly prepared powders showed reproducibly a smaller than previously reported hysteresis, of 2 K (Supporting Information Figure S2). The series with triflate as anion and increasing alkyl tails on the triazole (**7**−**10**) present similar transition temperatures around 220−230 K, and rather small residual HS fractions. Only compound **7** with pentyltriazole (m = 5) exhibits hysteresis with a width of 4 K. The transitions curves are comparatively more gradual with longer alkyl tails.[11] Compounds **11**, **12**, and **14**, obtained with formylaminotriazole, are sensible to water loss. Compound **11** possesses steep transitions with a hysteresis width of 2 K centered

dx.doi.org/10.1021/jp109489g |J. Phys. Chem. B 2011, 115, 3003–3012

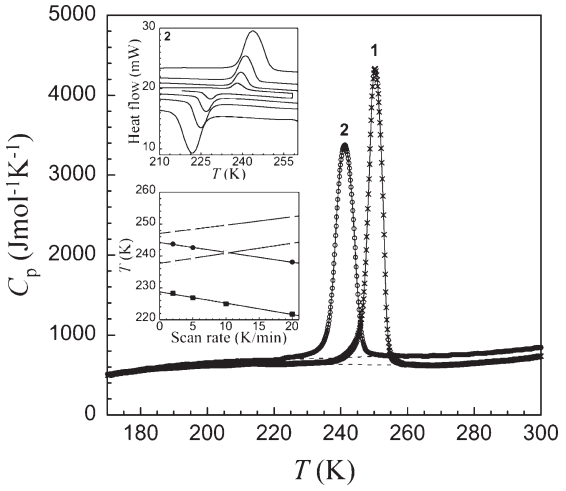

Figure 3. Molar heat capacities of compounds **1** (×) and **2** (○) upon warming at 10 K min^{-1}. Dash lines are estimated normal heat capacities used for ΔC_p determination. The insets represent cycles at various scan rates (20, 10, 5, and 2 K min^{-1}, endotherms are up) for **2** and the scan rate dependence of the maxima for both **1** (empty and full circles) and **2** (empty and full squares).

at 274 K, but if the temperature is increased above 340 K (under He atmosphere) more gradual transitions at lower temperatures are then observed.[9d] Compounds **12** (p-tol$^-$) and **14** (NO_3^-) are low spin at room temperature and experience a first LS→HS change at ca. 325 K, due to water loss and dictated by the kinetics of warming. The transition of the dehydrated species then occurs at lower temperatures with hysteresis of 5 and 10 K respectively. In **14**, a change of steepness occurs in the last stages of the first LS→HS change indicating a more complex mechanism (see Figure 8). Indeed, **12** reabsorbs spontaneously water in air at room temperature, while **14** remains dehydrated in the same conditions. The spin transition in **13** is centered at 283 K without hysteresis or any change of behavior after warming up to 380 K. All the transition temperatures, residual HS fractions, and ΔT_{80} are recalled in Table 1, together with those of the methoxyethyltriazole polymers **1**−**5**.

Thermal Properties. Calorimetric measurements have already been reported for $[Fe(fatrz)_3](CF_3SO_3)_2 \cdot 2H_2O$ (**11**),[9d] while the molar heat capacities at constant pressure, C_p, of the compounds with methoxyethyltriazole **1**-**5**, of **6** $[Fe(C_4trz)_3](BF_4)_2 \cdot 2H_2O$, of the series of triflate alkyltriazole polymers $[Fe(C_mtrz)_3](triflate)_2 \cdot 2H_2O$ (C_m = *n*-alkyl group with *m* C atoms, **7**, **8**, **9**, and **10** respectively with *m* = 5, 7, 10, 13),[24] and of compounds **12**-**14** deduced from DSC experiments are given respectively in Figures 3, 4, S3 (Supporting Information), 5, and 6′−8. Heat capacity anomalies are systematically observed at temperatures comparable to those of the SCO detected in magnetic properties with only some differences for compounds **4** and **12**, related to differences in sample environment as discussed in more details below (see Table 1). When relevant, experiments at variable scan-rates (see for example inset in Figure 3) confirm the presence of a hysteresis with similar widths as those observed in magnetic susceptibility data. The excess heat capacity, ΔC_p, due to the spin-crossover phenomenon in these materials is obtained by estimating a normal heat capacity curve with the high- and low-temperature data, which is represented as a dash line in the figures, and subtracting it from the total heat capacity. In this estimation, no

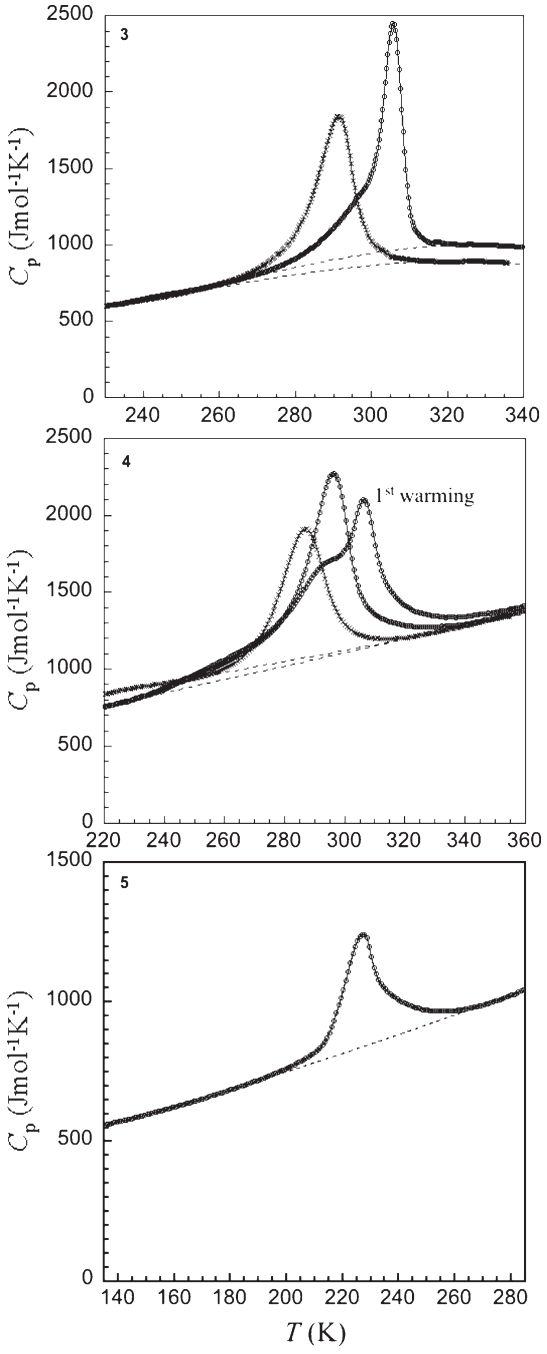

Figure 4. Molar heat capacities of compounds **3** (top), **4** (middle), and **5** (bottom) at 10 K min^{-1}. Empty circles and crosses respectively depict warming and cooling modes.

heat capacity step at the transition temperature was considered. The deduced calorimetric figures associated with the SCO $\Delta_{trans}H$ (integration of ΔC_p over T) and $\Delta_{trans}S$ (integration of ΔC_p over ln T) feature the observed difference in sharpness and are gathered in Table 1. The excess entropy values of all compounds considered here are much higher than the value that would arise from the change in spin state solely (R ln 5 = 13.4 J mol^{-1} K^{-1}), indicating a large vibrational entropy change upon the spin transition.

Compounds **1** and **2** (Figure 3) exhibit very sharp heat capacity anomalies, with large $\Delta_{trans}H$ and $\Delta_{trans}S$ values, as

dx.doi.org/10.1021/jp109489g |*J. Phys. Chem. B* 2011, 115, 3003–3012

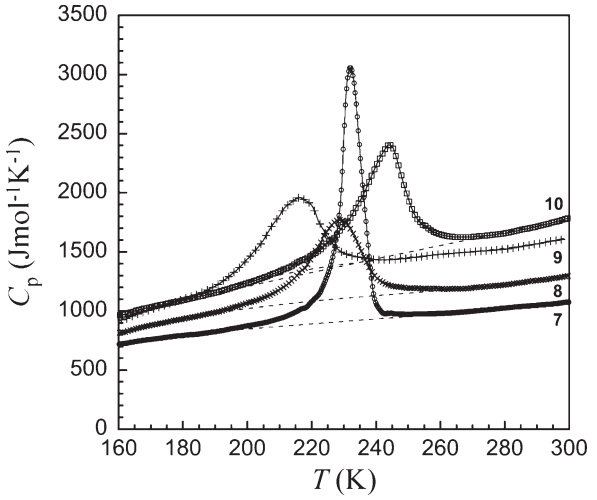

Figure 5. Molar heat capacities of the series $[Fe(C_mtrz)_3](CF_3SO_3)_2 \cdot 2H_2O$ (C_m = *n*-alkyl substituent with *m* C atoms) for *m* = 5 (○, 7), *m* = 7 (×, **8**), *m* = 10 (+, **9**) and *m* = 13 (□, **10**).

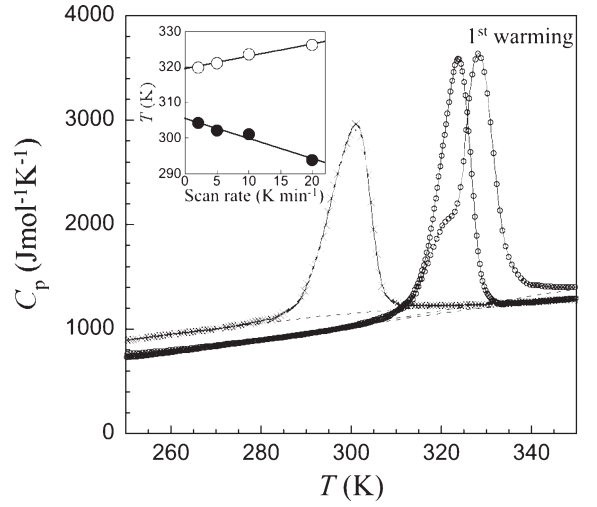

Figure 6. Molar heat capacities of compound **12** at 10 K min^{-1}. The first and subsequent stable warming measurements appear as empty circles (○) and crosses (×) represent the cooling mode. The inset shows the scan rate dependence of the peak maxima deduced from measurements at various rates.

opposed to the much broader anomaly displayed by compound **5** (Figure 4 bottom) with values of the order of what is found in gradual spin-transition systems. Indeed, the excess entropy for **5** is the smallest reported for such polymeric compounds. In agreement with the asymmetric appearance of the transition curves for the nitrate compound **3**, the C_p versus T curve upon warming exhibits a sharp anomaly around 306 K and a very broad tail at lower temperatures, while upon cooling a broader but simple peak is observed (Figure 4 top). This is an indication of inhomogeneities in transition temperatures: the main part of the sample has a well-defined transition corresponding to the sharp peak, but lower transition temperatures are also present, that can originate either in a slightly different environment of the Fe(II) ions or the presence of different interactions among the SCO centers.

The case of the p-tol$^-$ polymer **4** is peculiar. The first warming curve differs from the subsequent warmings (Figure 4 middle); it

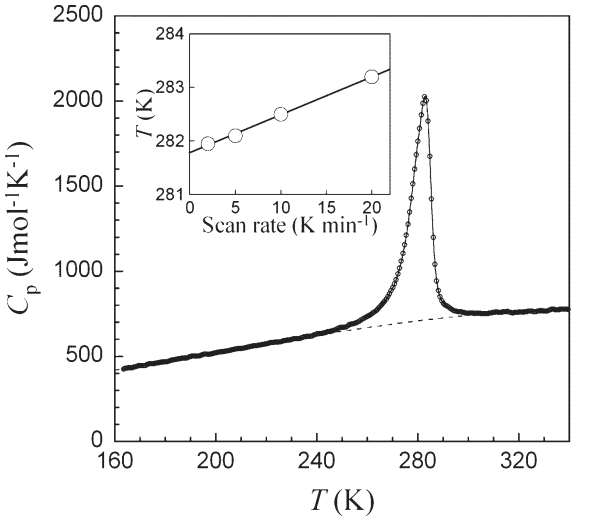

Figure 7. Molar heat capacities of compound **13** obtained upon warming at 10 K min^{-1}. The inset shows the scan rate dependence of the peak maximum deduced from measurements at various rates.

shows a main peak at higher temperatures, in addition to a first, smaller peak, at a temperature that matches the only peak observed in the subsequent warmings. These differences are related to the dehydration observed in TGA and magnetic data, but here an anomaly is also observed upon cooling at temperatures very close to those of the warming mode. Therefore, the DSC sample likely remains hydrated, as a consequence of the sealed aluminum pan used for the measurements. Most likely the differences between the first and the subsequent warmings arise from a rearrangement of the material to afford the water molecules that remain "trapped". The DSC sample indeed exhibits the same behavior as shown in Figure 2 bottom, if measured directly out of the sealed pan opened under inert atmosphere. Much higher enthalpies and entropies are derived in the warming measurements than in the cooling ones (Table 1), which has to be ascribed to a phenomenon other than the SCO occurring upon warming, and thus possibly related to a loss of water molecules. The rather large $\Delta_{trans}H$ and $\Delta_{trans}S$ found upon cooling are indeed comparable to that of compound **3** and other polymeric material of this type. It is therefore likely that, although the sample is not dehydrated, which would give an even higher enthalpy change, some kind of rearrangement involving the water molecules does occur during each warming cycle.

Similarly, in the case of **12** (Figure 6) the first and second warmings differ, but the peaks remain much higher in temperature than what was observed in magnetic measurements,[9d] without any change in sharpness. Indeed, a shoulder is detected in the first warming peak that exactly matches the position of the peak in the second warming. Since slightly higher entropy and enthalpy are found upon the first warming, and the temperature of the first warming peak corresponds to the first LS→HS spin change in the magnetic measurements, a rearrangement related to the water molecules probably occurs, but without dehydration, and therefore without a marked change in behavior. These properties can be ascribed to the hydrated form of **12**, as opposed to the magnetic properties that are characteristic of the dehydration of **12**, inducing a spin change. These differences crop up thanks to the sealed sample holder, which prohibits the evaporation of the water that the sample may loose. On the contrary, the DSC data for **14** is in good agreement with the magnetic data

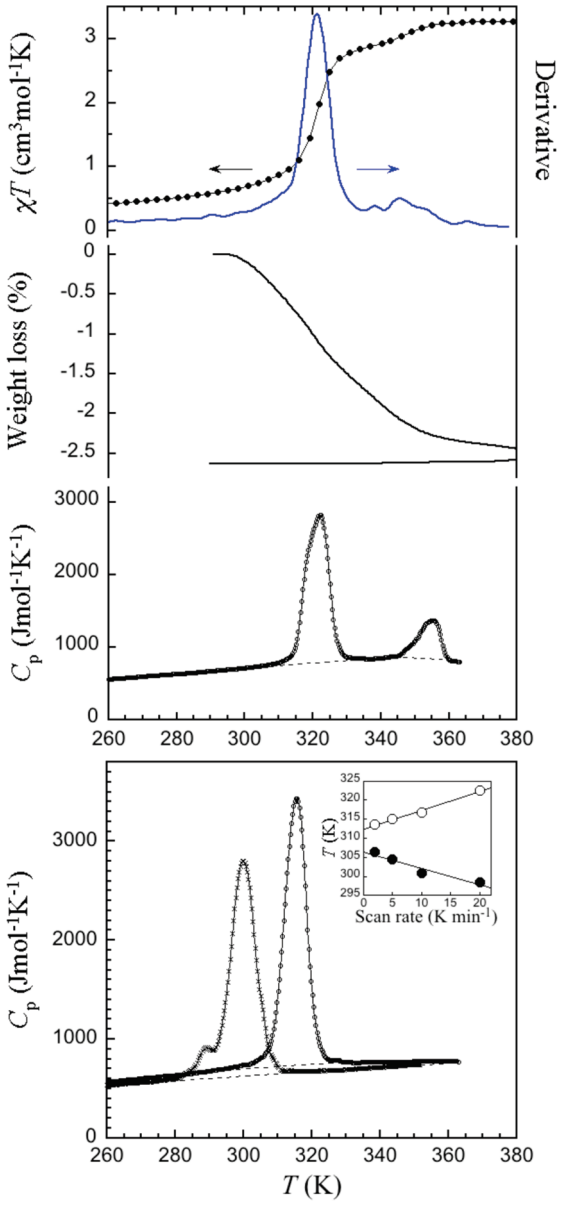

Figure 8. (Top) Magnetic, thermogravimetric, and DSC data for compound **14** upon the first warming. (Bottom) Molar heat capacities of compound **14** at 10 K min^{-1} after the first warming: empty circles (○) and crosses (×) represent respectively the stable warming and cooling modes. The inset shows the scan rate dependence of the peak maxima.

(Figure 8). Therefore, in the case of **14** dehydration does occur, even in the closed environment. Most probably, a rearrangement occurs upon dehydration that stabilizes the dehydrated form of **14**. Indeed the entropy associated with the second peak of the first warming, 11.8 J mol^{-1} K^{-1}, is rather small compared to an estimation of the entropy change of a simple dehydration process based on tabulated standard entropy data of hydrated compounds, that is, approximately 34 J mol^{-1} K^{-1}.

Importance of Water Content and Loss. Several works have already demonstrated the important role played by lattice water (or other protic solvent) molecules in SCO compounds,[25] and especially on $[Fe(Rtrz)_3](A)_2$ compounds,[9] through their effect on the ligand-field strength around the Fe(II) ions and therefore on $T_{1/2}$, as well as their prominent role as source of cooperativity through the building of H-bonding networks between SCO centers. In this frame, an additional interesting result brought about by the present calorimetric study is the indication of a different behavior of $[Fe(Rtrz)_3](p\text{-}tol)_2$ compounds when they are sealed. The dehydration process which is at the origin of the first spin change seems to be specific of these p-tol polymers. In general the dehydrated compound exhibits more gradual transitions at lower temperatures, which is mainly ascribed to the stabilization effect of the LS species by the water molecules. In many cases, spontaneous reabsorption in normal conditions in air occurs. In the absence of any humidity, the compound obviously remains dehydrated, as evidenced by the magnetic measurements performed in He atmosphere. Apparently, the dehydration process may also be affected by the conditions; in a sealed environment where the water molecules cannot evaporate, a spin transition is observed at high temperatures that cannot correspond to a dehydrated species. Two explanations may be put forward to account for the observed behavior: (i) dehydration does occur, but reabsorption of the water trapped in contact with the sample occurs at high temperatures and (ii) a rearrangement is induced to afford for the trapped water molecules upon the first warming and the subsequent behavior is that of these different hydrated species. The differences observed between the first warming DSC measurement and the subsequent warmings indeed seem to agree well with the latter hypothesis. However, if the sample is left in contact with air and submitted to the same series of measurements, exactly the same behavior is observed. Therefore, if a rearrangement occurs it is spontaneously reversible. In the case of compound **4** and **12**, spontaneous reabsorption of water occurs at room temperature in air, within minutes for **12** and within a day for **4**. Both dehydrated white compounds turn immediately purple when submitted to a water-saturated atmosphere. Upon dehydration, the sealed DSC pan (ca. 5 mm^3) would most likely contain such a wet atmosphere, and the first hypothesis is the most likely, at least in the two cases discussed here. In a more general manner however, none of the two proposed hypotheses can be discarded. The nitrate **14** indeed shows that if no reabsorption occurs, water may be trapped without affecting the properties of the dehydrated compound. Sealed polymeric p-tol compounds may be thought as additional sources of possible devices, since they allow different transition behavior. In the case of the triflate compound **11**, the use of sealed material simply assures that no dehydration will occur, and therefore the intrinsic transitions of the hydrated sample will remain usable as a temperature threshold indicator.[9d]

Calorimetric Figures and Cooperativeness of the Spin-Crossover. Rather sharp anomalies that are sometimes broadened have been detected in the heat capacity of the triazole-based polymeric SCO compounds studied here and in the past. These anomalies are directly related to the change in spin state and the vibrational changes induced in the sample. The excess enthalpies and entropies derived are systematically higher than in typical cooperative mononuclear SCO compounds; with the exception of **5**, the excess enthalpies are higher than 10 kJ mol^{-1} and the vibrational entropies higher than 35 J mol^{-1} K^{-1}. The corresponding strong cooperative behavior of these materials is most likely to be related to the direct rigid chemical link between the iron(II) centers afforded by the triple N1,N2-triazole bridges. However, even compounds with a gradual transition/large ΔT_{80} gave large enthalpies and entropies. Therefore, a quantified measure of the cooperativity appears necessary,

to compare with the thermodynamic parameters. For this purpose, we have considered two widely used models in SCO materials: (i) the so-called Slichter and Drickamer model,[26] that uses a mean-field interaction term Γ (see Supporting Information eq S1) and (ii) the phenomenological domain model proposed by Sorai[4] that measures the cooperativity through the number n of like-spin centers per interacting domain (Supporting Information eq S2). The experimental HS fractions calculated from magnetic measurements[27] were fit to both models, fixing the thermodynamic figures to the ones determined by DSC calorimetry (except for compounds **4** and **12**). Figure 9 presents the results for compound **1**, as an example, while more details are given in the Supporting Information. The warming branch of the hysteresis curves have also been fit to the Slichter and Drickamer model (inset in Figure 9), the resulting Γ being coined Γ_{up}, to allow a comparison of the two models (the domain model cannot reproduce hysteretic behaviors) as well as the steepness of the SCO curves of compounds with and without hysteresis.[28] The results are gathered in Table 1.

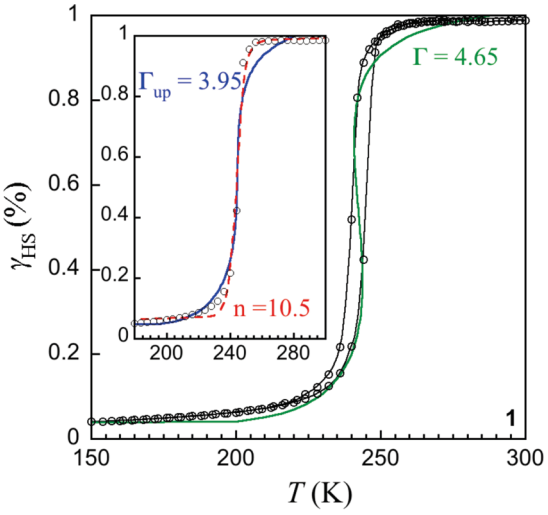

Figure 9. The spin crossover of compound **1** shown as the high-spin fraction γ_{HS} vs T,[27] and its simulation with the Slichter and Drickamer model (green and blue full lines) and the domain model (red dashed line), as described in the text. The inset shows only the warming branch of the SCO curve. Values of Γ are given in kJ mol^{-1}.

The same procedure was applied to similar one-dimensional triazole-based SCO compounds for which both accurate calorimetric data (either from DSC or adiabatic calorimetry) and magnetic and/or optical data allowing to determine a γ_{HS} versus T curve are available in the literature, namely $[Fe(Htrz)_2(trz)](BF_4)\cdot H_2O$,[15,29] $[Fe(hyptrz)_3](ncbs)_2\cdot 2H_2O$,[30] $[Fe(tba)_3](A)_2\cdot 3H_2O$ (A = BF_4^- and p-tol$^-$) and $[Fe(tba)_3](CF_3SO_3)_2$,[31] $[Fe(Htrz)_3](B_{10}H_{10})\cdot H_2O$,[32] $[Fe(C_3trz)_3](CF_3SO_3)_2\cdot 5H_2O$ and $[Fe(C_3trz)_3]Br_2\cdot 4H_2O$,[33] $[Fe(atrz)_3](ReO_4)_2$ and $[Fe(atrz)_3]SiF_6\cdot H_2O$,[34] and $[Fe(atrz)_3](A)_2$ (A = Br$^-$ and ClO_4^-).[35] The parameters describing their SCO process and the results of the fits to Supporting Information eqs S1 and S2 are listed in Table 2. For values of $\Gamma/RT_{SCO} > 2$ in the Slighter and Drickamer model, a bistability is predicted, and the width of the resulting hysteresis in the SCO curve increases with Γ/RT_{SCO}. The family of related SCO compounds considered here provides a good experimental verification, shown in Figure 10.

The origin of cooperativity in SCO solids is the interaction between the SCO centers. Γ is a phenomenological measure of this interaction and thus of cooperativity and has a similar meaning as the interaction J in the Ising model applied to the SCO phenomenon with $\Gamma/2R = zJ$. On the other hand, the number of centers having correlated electronic states given by the domain model, n, is an indirect measure of the actual interaction. A relation between this macroscopic parameter n and the parameters of a microscopic model of the interaction among SCO centers has previously been derived.[36] Because the domain model cannot reproduce hysteresis, n can only be compared to Γ_{up}, as done in Supporting Information Figure S4. Quite

Table 2. Transition Temperatures, Abruptness of Transition Curve, and Measured Excess Enthalpies and Entropies Due to the Spin Transition in Related 1D Triazole-Based Compounds

compound	T_{SCO} (K)[a]	$T_{1/2}^{up}$ (K)	$T_{1/2}^{down}$ (K)	ΔT_{80} (K)	res HS (%)	$\Delta_{trans}H$ (kJ mol^{-1})[b]	$\Delta_{trans}S$ (J mol^{-1} K^{-1})[b]	Γ/Γ_{up} (kJmol^{-1})	n	ref
$[Fe(Htrz)_2(trz)](BF_4)\cdot H_2O$ a	365	385	345	3	<1	27.8	75	10.00/6.50	49.8	15
$[Fe(Htrz)_2(trz)](BF_4)\cdot H_2O$ b	333	343	323	8	5	22.5	77	7.25/5.60	17.9	15
$[Fe(Htrz)_2(trz)](BF_4)\cdot H_2O$	357	371	343	3.5	2	26.6	72	8.55/6.15	51.0	29
$[Fe(hyptrz)_3](ncbs)_2\cdot 2H_2O$	144	168	120	30	25	7.3	42.4	4.35/2.65	8.6	30
$[Fe(tba)_3](BF_4)_2\cdot 3H_2O$	254	258	250	10	1	17.8	67.2	5.08/4.30	12.1	31
$[Fe(tba)_3](p\text{-}tol)_2\cdot 3H_2O$	232	238	226	17	5	14.6	63.5	4.75/3.65	6.2	31
$[Fe(tba)_3](CF_3SO_3)_2$	296.5	309	284	27	1	19.7	65.6	6.15/4.60	9.9	31
$[Fe(Htrz)_3](B_{10}H_{10})\cdot H_2O$	239.5	246	233	60	2	10.1	43	4.40/2.75	3.9	32
$[Fe(C_3trz)_3](CF_3SO_3)_2\cdot 5H_2O$	204.5	207	202	20	2	11.2	56.5	3.75/3.15	8.3	33
$[Fe(C_3trz)_3]Br_2\cdot 4H_2O$	249.5	252	247	12	2	18.8	73.9	4.40/2.75	13.3	33
$[Fe(atrz)_3](ReO_4)_2$	228	228	228	85	18	7.3	32.8	2.65	3.9	34
$[Fe(atrz)_3]SiF_6\cdot H_2O$	255	255		7	31	11.4	45.6	5.05/4.20	40.4	34
$[Fe(atrz)_3]Br_2$	323	328	318	19	1	22.3	67.6	6.35/5.10	10.6	35
$[Fe(atrz)_3](ClO_4)_2$	165	165	165	120	30	4.4	30	1.90	3.8	35

[a] $T_{1/2}$ stands for the temperature at which half of the SCO centers have change their spin; for comparison of compounds with and without hysteresis, T_{SCO} is defined as $(T_{1/2}^{up} + T_{1/2}^{down})/2$. [b] Excess enthalpies and entropies are given per mole of transition Fe(II) ions: they are corrected of the residual HS fraction evaluated through UV-vis-NIR spectroscopy at low temperature.

dx.doi.org/10.1021/jp109489g |J. Phys. Chem. B 2011, 115, 3003–3012

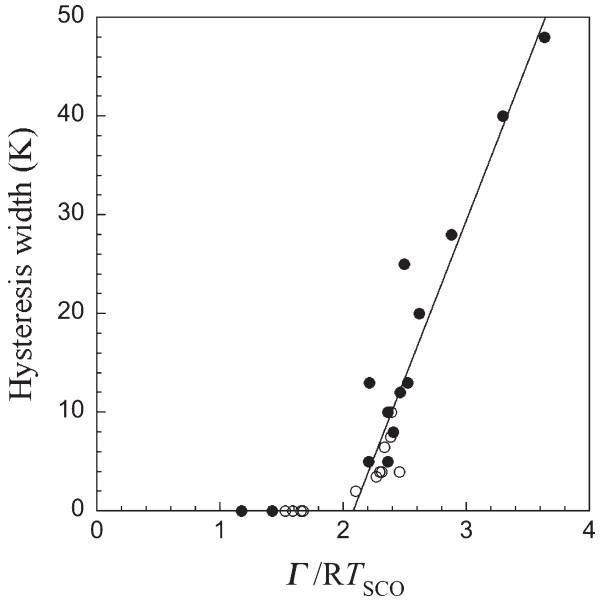

Figure 10. Correlation of the hysteresis width observed in experimental SCO curves with the cooperativity parameter, Γ/RT_{SCO}. Empty symbols correspond to compound of the present work, while full symbols correspond to SCO compound taken from literature (see Table 2). The full line is a linear fit of the data for $\Gamma/RT_{SCO} > 2$.

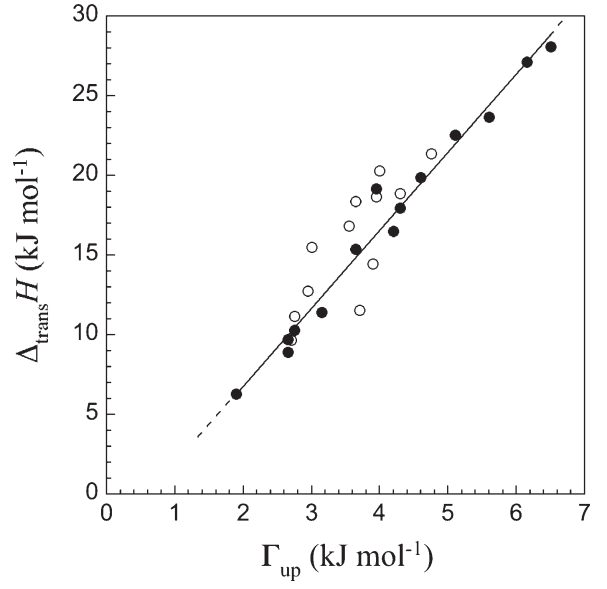

Figure 11. Correlation of the excess enthalpy involved in the SCO $\Delta_{trans}H$ and the phenomenological cooperativity parameter Γ_{up}. Empty symbols correspond to compounds of the present work, while full symbols correspond to SCO curves taken from literature (see Table 2). The full line is a linear fit of all data, with equation $\Delta_{trans}H = -3.09 + 4.90\ \Gamma_{up}$.

satisfactorily the two models are correlated with a linear decrease of $\Gamma_{up}/RT_{1/2}{}^{up}$, the "cooperativity", with the inverse of n.

More importantly the experimental excess enthalpy associated with the SCO process is found to correlate with both Γ_{up} (Figure 11) and n (Supporting Information Figure S5).[28] Interestingly, it is also found to correlate with $\Delta T_{80}/T_{SCO}$ (Supporting Information Figure S6), a purely experimental measure of the abruptness of the SCO curves and therefore of cooperativity, thus supporting that found with the parameters of the two models used. This is important since one has to keep in mind that due to the polymeric nature of the materials, the derived values of Γ and n are likely average values describing the consequence of a distribution in size of polymeric chains. The linear correlation of $\Delta_{trans}H$ with Γ_{up} is particularly good, and therefore allows to consider the experimental determination of $\Delta_{trans}H$ from calorimetric measurements as a direct experimental quantitative determination of the cooperative character of the SCO. Obviously this correlation is valid only for the triazole-based family of compounds considered here. Similar correlations would probably be derived if other large families of SCO compounds with similar solid structures could be made. On the other hand, the correlation of the excess entropy $\Delta_{trans}S$ with the variation in cooperativity is much poorer, as shown in Supporting Information Figure S7. Large values are found for all compounds of the triazole-based series, and there is no evident relation with any of the parameters describing the cooperative character of the SCO (ΔT_{80}, Γ, n, hysteresis width). Therefore a large excess entropy should not be used as a measure of cooperativity in SCO solids, as has been done qualitatively so far.

CONCLUSION

The cooperative character of the spin-crossover of $[Fe(Rtrz)_3](A)_2$ coordination polymers has been quantified with the phenomenological so-called Slichter and Drickamer and domain models for various series of 4-substituent R, the one with R = methoxyethyl being reported here for the first time. Thermodynamic figures associated with the SCO process in these materials have been systematically determined by calorimetric measurements or taken from literature when available. The experimental excess enthalpy arising from the SCO is directly correlated with the parameters derived from both models used, thus providing a direct experimental quantitative evaluation of the cooperativity in these widely studied SCO materials. Instead of the excess entropy for which no such clear correlation is observed, the excess enthalpy should preferably be used as a measure of the cooperativity in SCO compounds.

ASSOCIATED CONTENT

Supporting Information. UV−vis absorption spectra, χT vs T plot and molar heat capacities of compound **6**, details of fitting of transition curves, and additional correlation plots. This material is available free of charge via the Internet at http://pubs.acs.org.

AUTHOR INFORMATION

Corresponding Author

*E-mail: roubeau@unizar.es. Tel.: +34 976 76 2461. Fax: +34 976 76 1229.

ACKNOWLEDGMENT

The work described was supported by the Leiden University Study group WFMO (Werkgroep Fundamenteel Materialen-Onderzoek), the CSIC (PIE to OR), and the Spanish MICINN and FEDER through project MAT2007-61621.

REFERENCES

(1) (a) Carlin, R. L. *Magnetochemistry*; Springer-Verlag: Berlin, 1986. (b) Sorai, M.; Nakano, M.; Miyazaki, Y. *Chem. Rev.* **2006**, *106*, 976–1031.

(2) (a) *Top. Curr. Chem.* 2004, 233−235; Gütlich, P.; Goodwin, H. A., Eds. (b) Gütlich, P. *Struct. Bonding (Berlin, Ger.)* **1981**, *44*, 83–195. (c) Gütlich, P.; Garcia, Y.; Goodwin, H. A. *Chem. Soc. Rev.* **2000**, *29*, 419–427. (d) Gütlich, P.; Hauser, A.; Spiering, H. *Angew. Chem., Int. Ed. Engl.* **1994**, *33*, 2024–2054.

(3) Kahn, O.; Kröber, J.; Jay, C. *Adv. Mater.* **1992**, *4*, 718–728.

(4) (a) Sorai, M.; Seki, S. *J. Phys. Chem. Solids* **1974**, *35*, 555–570. (b) Sorai, M. *Top. Curr. Chem.* **2004**, *235*, 153–170.

(5) (a) König, E. *Prog. Inorg. Chem.* **1987**, *35*, 527–622. (b) Guionneau, P.; Marchivie, M.; Bravic, G.; Létard, J.-F.; Chasseau, D. *Top. Curr. Chem.* **2004**, *234*, 97–128.

(6) Spiering, H. *Top. Curr. Chem.* **2004**, *235*, 171–195 and references therein.

(7) Kaji, K.; Sorai, M. *Thermochim. Acta* **1985**, *88*, 185–190.

(8) See for example: (a) Sorai, M.; Nagano, Y.; Conti, A. J.; Hendrickson, D. N. *J. Phys. Chem. Solids* **1994**, *55*, 317–326. (b) Nakamoto, N.; Tan, Z. C.; Sorai, M. *Inorg. Chem.* **2001**, *40*, 3805–3809. (c) Roubeau, O.; de Vos, M.; Stassen, A. F.; Burriel, R.; Haasnoot, J. G.; Reedijk, J. *J. Phys. Chem. Solids* **2003**, *64*, 1003–1013.

(9) (a) Kahn, O.; Codjovi, E. *Philos. Trans. R. Soc. London , Ser. A* **1996**, *354*, 359–379. (b) Kahn, O.; Martinez, C. J. *Science* **1998**, *279*, 44–48. (c) Garcia, Y.; van Konningsbruggen, P. J.; Lapouyade, R.; Fournès, L.; Rabardel, L.; Kahn, O.; Ksenofontov, V.; Levchenko, G.; Gütlich, P. *Chem. Mater.* **1998**, *10*, 2426–2433. (d) Roubeau, O.; Haasnoot, J. G.; Codjovi, E.; Varret, F.; Reedijk, J. *Chem. Mater.* **2002**, *14*, 2559–2566.

(10) (a) Roubeau, O.; Colin, A.; Schmitt, V.; Clérac, R. *Angew. Chem., Int. Ed.* **2004**, *43*, 3283–3286. (b) Fujigaya, T.; Jiang, D.-L.; Aida, T. *Chem. Asian J.* **2007**, *2*, 106–113. (c) Roubeau, O.; Natividad, E.; Agricole, B.; Ravaine, S. *Langmuir* **2007**, *23*, 3110–3117. (d) Roubeau, O.; Agricole, B.; Clérac, R.; Ravaine, S. *J. Phys. Chem. B* **2004**, *108*, 15110–15116. (e) Coronado, E.; Galán-Mascarós, J. R.; Monrabal-Capilla, M.; García-Martínez, J.; Pardo-Ibáñez, P. *Adv. Mater.* **2007**, *19*, 1359–1361. (f) Forestier, T.; Mornet, S.; Daro, N.; Nishihara, T.; Mouri, S-I; Tanaka, K.; Fouché, O.; Freysz, E.; Létard, J.-F. *Chem. Commun.* **2008**, 432–4329.

(11) Roubeau, O.; Alcazar Gomez, J. M.; Balskus, E.; Kolnaar, J. J. A.; Haasnoot, J. G.; Reedijk, J. *New J. Chem.* **2001**, *25*, 144–150.

(12) (a) Lavrenova, L. G.; Ikorskii, V. N.; Varnek, V. A.; Oglezneva, I. M.; Larionov, S. V. *Koord. Khim.* **1986**, *12*, 207. (b) Varnek, V. A.; Lavrenova, L. G. *J. Struct. Chem.* **1995**, *36*, 104–111. (c) Dîrtu, M. M.; Rotaru, A.; Gillard, A.; Linarès, J.; Codjovi, E.; Tinant, B.; Garcia, Y. *Inorg. Chem.* **2009**, *48*, 7838–7852.

(13) (a) Michalowicz, A.; Moscovici, J.; Ducourant, B.; Cracco, D.; Kahn, O. *Chem. Mater.* **1995**, *7*, 1833–1842. (b) Michalowicz, A.; Moscovici, J.; Kahn, O. *J. Phys. IV* **1997**, *7*, C2-633–635. (c) Verelst, M.; Sommier, L.; Lecante, P.; Mosset, A.; Kahn, O. *Chem. Mater.* **1998**, *10*, 980–985.

(14) (a) Garcia, Y.; van Koningsbruggen, P. J.; Bravic, G.; Guionneau, P.; Chasseau, D.; Cascarano, G. L.; Moscovici, J.; Lambert, K.; Michalowicz, A.; Kahn, O. *Inorg. Chem.* **1997**, *36*, 6357–6365. (b) Drabent, K.; Ciunik, Z. *Chem. Commun.* **2001**, 1254–1255. (c) Garcia, Y.; van Koningsbruggen, P. J.; Bravic, G.; Chasseau, D.; Kahn, O. *Eur. J. Inorg. Chem.* **2003**, 356–362.

(15) Kröber, J.; Audière, J. P.; Claude, R.; Codjovi, E.; Kahn, O.; Haasnoot, J. G.; Grolière, F.; Jay, C.; Bousseksou, A.; Linarès, J.; Varret, F.; Gonthier-Vassal, A. *Chem. Mater.* **1994**, *6*, 1404–1412.

(16) (a) Linarès, J.; Spiering, H.; Varret, F. *Eur. J. Phys. B* **1999**, *10*, 271–275. (b) Boukheddaden, K.; Linarès, J.; Spiering, H.; Varret, F. *Eur. Phys. J. B* **2000**, *15*, 317–326.

(17) Bayer, H. O.; Cook, R. S.; von Mayer, W. C. U.S. Patent 3,821,376, 1974.

(18) Kahn, O. *Molecular Magnetism*; VCH Publishers: New York, 1993.

(19) Sarge, S. M.; Hemminger, W.; Gmelin, E.; Höhne, G. W. H.; Cammenga, H. K.; Eysel, W. J. *J. Therm. Anal.* **1997**, *49*, 1125–1234.

(20) (a) Vos, G.; Le Fêbre, R. A.; de Graaf, R. A. G.; Haasnoot, J. G.; Reedijk, J. *J. Am. Chem. Soc.* **1983**, *105*, 1682–1683. (b) Kolnaar, J. J. A.; van Dijk, G.; Kooijman, H.; Spek, A. L.; Ksenofontov, V.; Gütlich, P.; Haasnoot, J. G.; Reedijk, J. *Inorg. Chem.* **1997**, *36*, 2433–2440.

(21) Sugiyarto, K. H.; Goodwin, H. A. *Aust. J. Chem.* **1994**, *47*, 263–277.

(22) Grondin, P.; Roubeau, O.; Castro, M.; Saadaoui, H.; Colin, A.; Clérac, R. *Langmuir* **2010**, *26*, 5184–5195.

(23) Codjovi, E.; Sommier, L.; Kahn, O.; Jay, C. *New J. Chem.* **1996**, *20*, 503–505.

(24) A first measurement of the heat capacity of $[Fe(pentyltrz)_3](CF_3SO_3)_2 \cdot 2H_2O$ (**7**) was performed earlier (ref 11), by use of a relaxation technique (heat capacity option of a Quantum Design PPMS6000). The transitions were observed at temperatures in good agreement with the magnetic measurements, but the calorimetric figures deduced were found much lower than with DSC here ($\Delta H = 5.3$ J mol^{-1} and $\Delta S = 24.7$ J mol^{-1} K^{-1}). Unfortunately, the amount of sample used was at the bottom margin of the setup, and the quality of the data at high temperatures was poor. This made the determination of a normal heat capacity curve difficult, if not incorrect, probably at the origin of the discrepancy observed.

(25) (a) Sorai, M.; Ensling, J.; Hasselbach, K. M.; Gütlich, P. *Chem. Phys.* **1977**, *20*, 197–208. (b) Buchen, T.; Gütlich, P.; Sugiyarto, K. H.; Goodwin, H. A. *Chem.—Eur. J.* **1996**, *2*, 1134–1138. (c) Gütlich, P.; Köppen, H.; Steinhaüser, H. G. *Chem. Phys. Lett.* **1980**, *74*, 475–480. (d) Salmon, L.; Donnadieu, B.; Bousseksou, A.; Tuchagues, J.-P. *C. R. Acad. Sci. Paris II, Sér. C* **1999**, *2*, 305–309.

(26) Slichter, C. P.; Drickamer, H. *J. Chem. Phys.* **1972**, *56*, 2142–2161.

(27) The HS fraction γ_{HS} was deduced from the magnetic data using the relation $\gamma_{HS} = (\chi T - \chi T_{LS})/(\chi T_{HS} - \chi T_{LS})$, where χT_{LS} and χT_{HS} stand respectively for the values of χT in the LS and HS states. Equations S1 and S2 were thus fitted to an effective γ_{HS} not including the nontransiting residual HS fraction, indicated by large values of χT_{LS} and evaluated through UV-vis-NIR spectroscopy at low temperature.

(28) Another reason to model the warming branch of the compounds with hysteresis is that the correlation is intended with calorimetric figures that are determined upon warming. Moreover, in the present compounds it is possible that secondary rearrangements triggered by the spin transition participate in the observation of hysteresis, since for some compounds gradual SCO curves do show hysteresis. In this frame, it is not incorrect to use a mean-field model on only one branch of the hysteresis.

(29) Cantin, C.; Kliava, J.; Marbeuf, A.; Mikaïlitchenko, D. *Eur. Phys. J. B* **1999**, *12*, 525–540.

(30) Garcia, Y.; Moscovici, J.; Michalowicz, A.; Ksenofontov, V.; Levchenko, G.; Bravic, G.; Chasseau, D.; Gütlich, P. *Eur. J. Inorg. Chem.* **2002**, 4992–5000.

(31) Seredyuk, M.; Gaspar, A. B.; Muñoz, M. C.; Verdaguer, M.; Villain, F.; Gütlich, P. *Eur. J. Inorg. Chem.* **2007**, 4481–4491.

(32) Berezovskii, G. A.; Bushuev, M. B.; Pishchur, D. P.; Lavrenova, L. G. *J. Therm. Anal. Calorim.* **2008**, *93*, 999–1002.

(33) Berezovskii, G. A.; Bushuev, M. B.; Lavrenova, L. G. *Russ. J. Phys. Chem.* **2004**, *78*, 1708–1711.

(34) Berezovskii, G. A.; Shakirova, O. G.; Svedenkov, Y. G.; Lavrenova, L. G. *Russ. J. Phys. Chem.* **2003**, *77*, 1054–1058.

(35) Berezovskii, G. A.; Bessergenev, Y. G.; Lavrenova, L. G.; Ikorskii, V. N. *Russ. J. Phys. Chem.* **2002**, *76*, 1246–1250.

(36) Nishino, M.; Miyashita, S.; Boukheddaden, K. *J. Chem. Phys.* **2003**, *118*, 4594–4597.